CO2 fluxes across the air-sea interface in the southeastern Beaufort Sea: Ice-free period

Alfonso Mucci, Bruno Lansard, Lisa Miller, Timothy Papakyriakou

JOURNAL OF GEOPHYSICAL RESEARCH, VOL. 115, C04003, doi:10.1029/2009JC005330, 2010

CO_2 fluxes across the air-sea interface in the southeastern Beaufort Sea: Ice-free period

Alfonso Mucci,[1] Bruno Lansard,[1] Lisa A. Miller,[2] and Timothy N. Papakyriakou[3]

Received 13 February 2009; revised 7 September 2009; accepted 13 November 2009; published 1 April 2010.

[1] Surface mixed layer CO_2 fugacities (fCO_2-sw) calculated from carbonate system parameters in the southeastern Beaufort Sea during the ice-free period ranged from 240 to 350 μatm in fall 2003 and from 175 to 515 μatm in summer 2004. The surface mixed layer remains mostly undersaturated with respect to atmospheric CO_2 (378 μatm) and, therefore, acts as a potential CO_2 sink throughout this period. Air-sea CO_2 fluxes (FCO_2) were first computed assuming ice-free conditions and ranged from −32.4 to +8.6 mmol m^{-2} d^{-1} in fall 2003 and summer 2004, respectively. Then we included a reduction factor to account for ice cover (ic) and we computed the resulting fluxes (FCO_2-ic). In fall 2003, FCO_2-ic ranged from −4.7 mmol m^{-2} d^{-1} in the relatively open water of the Cape Bathurst Polynya to −0.1 mmol m^{-2} d^{-1} in the southeastern Beaufort Sea, limited by the presence of the multiyear sea ice. In summer 2004, FCO_2-ic ranged from −13.1 mmol m^{-2} d^{-1} on the western Mackenzie Shelf to +8.6 mmol m^{-2} d^{-1} at Cape Bathurst; the variability being ascribed to competing effects of vertical mixing, temperature variations, and possibly biological production. On average, a net sink of −2.3 ± 3.5 mmol m^{-2} d^{-1} was estimated for the ice-free period over the study area. Nevertheless, the FCO_2 displays strong variability due to ice coverage, freshwater input, and upwelling events. The potential responses (direction and intensity of potential feedbacks) of the carbon cycle in the study area to a changing Arctic climate are discussed.

Citation: Mucci, A., B. Lansard, L. A. Miller, and T. N. Papakyriakou (2010), CO_2 fluxes across the air-sea interface in the southeastern Beaufort Sea: Ice-free period, *J. Geophys. Res.*, *115*, C04003, doi:10.1029/2009JC005330.

1. Introduction

[2] Models predict that global climate change will accelerate under the most probable CO_2 emission scenarios, and that the greatest effects will be felt in the northern polar region [*Hassol*, 2004; *Intergovernmental Panel on Climate Change*, 2008]. Recent satellite and field observations of the Arctic Ocean have revealed a steadily decreasing ice cover with recent summer months setting new record lows in ice concentration [*Serreze et al.*, 2007; *Stroeve et al.*, 2007; *Comiso et al.*, 2008]. Similar trends have also been reported with respect to ice thickness during the winter months [*Laxon et al.*, 2003; *Yu et al.*, 2004]. A receding ice cover and direct exposure of the air-sea interface will probably result in more efficient gas exchange with the atmosphere [*Bates et al.*, 2006]. Furthermore, whereas ice algal production contributes significantly to the total primary productivity in the central Arctic [*Gosselin et al.*, 1997], the greater light penetration in the absence of sea ice cover should normally lead to increased primary productivity. In this context, the Arctic Ocean may play a greater role as an anthropogenic CO_2 sink.

[3] Conversely, increasing river flow and freshwater inputs, in response to global warming [*Peterson et al.*, 2006], could decrease the CO_2 sink. The Arctic Ocean receives an estimated 3 300 km^3 y^{-1} of freshwater through river discharge. Rivers flowing into the Arctic Ocean drain 14 × 10^6 km^2 of northern Asia, northern Europe and North America [*Stein*, 2000]. The impact of increased river flow on primary productivity in the coastal Arctic Ocean is difficult to predict since, while the delivery of terrestrial nutrients will likely increase, stratification will also likely increase, limiting the flux of nutrients into the surface waters from depth [*Carmack et al.*, 2004]. In addition, the input of suspended particulate matter to the coastal ocean may impede primary productivity by limiting light penetration, while the greater delivery of allochthonous organic matter, amplified by permafrost melting in subarctic and arctic catchments [*Payette et al.*, 2004], may lead to increased organic carbon respiration and a net source of metabolic CO_2 in coastal waters. Decreasing ice formation and cover could also reduce the sink of atmospheric CO_2, if stratification is reduced due to less ice melt and increased wind stress, promoting upwelling and bringing CO_2-rich waters up to the surface [*Pipko et al.*, 2002; *Bates*, 2006; *Semiletov et al.*, 2007]. Whether these changes arise as a result of natural

[1]GEOTOP, Department of Earth and Planetary Sciences, McGill University, Montreal, Quebec, Canada.
[2]Centre for Ocean Climate Chemistry, Institute of Ocean Sciences, Fisheries and Oceans Canada, Sidney, British Columbia, Canada.
[3]Centre for Earth Observation Science, Department of Environment and Geography, University of Manitoba, Winnipeg, Manitoba, Canada.

0148-0227/10/2009JC005330

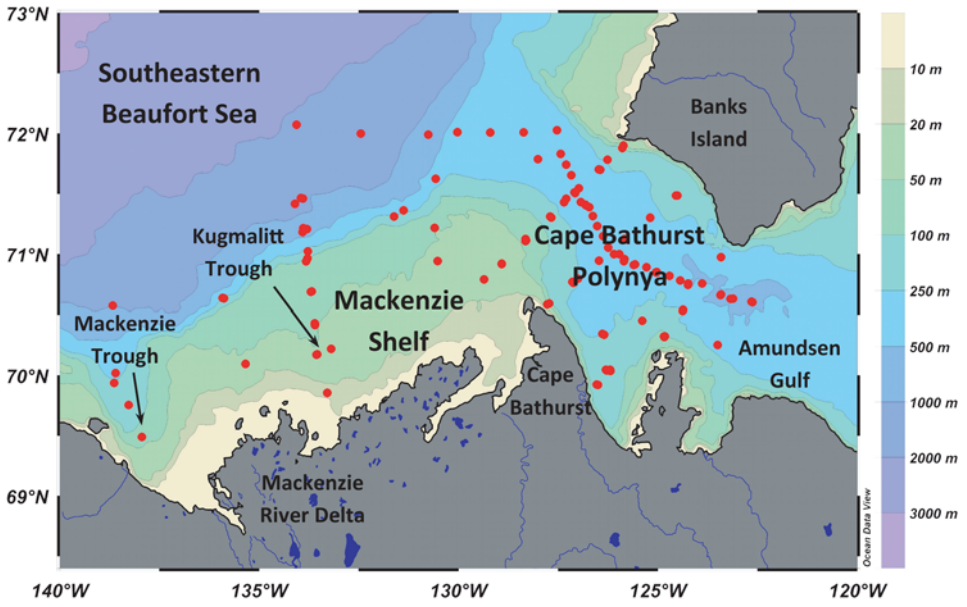

Figure 1. Map of the CASES study area showing the bathymetry and the location of the sampling stations covered by the CCGS *Amundsen* in fall 2003 and summer 2004. The three physiographic regions discussed in this paper are indicated.

cycles [*Venegas and Mysak*, 2000] or global warming [*Johannessen et al.*, 1996; *Shindell et al.*, 1999], the response of the carbon cycle in polar regions to such changes is critical in determining the direction and intensity of potential feedbacks [*McGuire et al.*, 2009].

[4] This study focuses on the western Canadian Arctic Archipelago, specifically the southeastern Beaufort Sea encompassing the Mackenzie Shelf, the Cape Bathurst Polynya and the Amundsen Gulf, an area which has displayed alarming increases in surface temperature over the last few decades [*Comiso*, 2003] as well as a steady decrease in ice concentration since the early 1980s [*Barber and Hanesiak*, 2004; *Galley et al.*, 2008]. The Mackenzie River is the largest single source of sediment to the Arctic Ocean [*Carson et al.*, 1998; *Macdonald et al.*, 1998]. Of the 250 × 10^9 kg y^{-1} of suspended particulate matter delivered by all rivers to the Arctic Ocean, the Mackenzie River discharges 118 to 127 × 10^9 kg y^{-1} of sediments and approximately 3 × 10^9 kg y^{-1} of dissolved and particulate organic carbon to the Beaufort Sea [*Droppo et al.*, 1998; *Macdonald et al.*, 1998]. Consequently, land-derived organic carbon accounts for the majority of the organic matter in Beaufort Shelf sediments [*Goñi et al.*, 2005; *Yunker et al.*, 2005]. Although coastal erosion provides an additional source of allochthonous organic carbon to the Mackenzie Shelf, its contribution (~7%) is minimal [*Macdonald et al.*, 1998].

[5] In this study, we report fCO_2-sw in the surface mixed layer (SML) from which we estimate fluxes at the air-sea interface in the southeastern Beaufort Sea during the largely ice-free seasons of the Canadian Arctic Shelf Exchange Study (CASES) program: September–November 2003 and June–August 2004. Most of the freshwater discharge from the Mackenzie River occurs during this period, i.e., May–October [*Carmack and Macdonald*, 2002]. These data serve to establish whether seasonal variations in surface fCO_2-sw can be associated with the hydrological cycle (Mackenzie River inputs, sea ice formation versus melting) or the onset of phytoplankton blooms, as well as to estimate the strength of the CO_2 sink in this region of the Arctic Ocean.

2. Methods

2.1. Water Column Chemistry of the Carbonate System

[6] Seawater samples were collected at numerous stations throughout the water column in the southeastern Beaufort Sea, the Cape Bathurst Polynya and on the Mackenzie Shelf (Figure 1), between September 2003 and August 2004, onboard the icebreaker CCGS Amundsen (Table 1). Water samples were recovered using a rosette sampling system equipped with 24 × 12 L Niskin bottles, a CTD (SBE 911plus) and a Seapoint fluorometer. The temperature probe was calibrated by the manufacturer, and the conductivity sensor was calibrated using discrete salinity samples taken almost daily throughout the water column and analyzed on a Guildline Autosal 8400 salinometer calibrated with IAPSO standard seawater. The output of the CTD fluorometer was calibrated against chlorophyll-*a* (Chl *a*) concentrations measured on discrete samples taken between April and August 2004. The fluorometer signal was fitted to a quadratic polynomial equation: Chl a = −0.035 + (1.871 × Fluo) − (0.134 × ($Fluo^2$)) and revealed that the fluorescence yield of Chl *a* decreased with increasing biomass [*Tremblay et al.*, 2008]. Water samples for dissolved inorganic carbon (DIC) and total alkalinity (TA) analysis were transferred to separate 500 mL glass bottles using standard protocols [*Dickson and Goyet*, 1994] as soon as the rosette was secured onboard. Headspace gas, equivalent to 1% of the bottle volume was set reproducibly using a machined Teflon plunger, and 100 μL of a saturated $HgCl_2$ solution were added before the bottle was sealed with a ground glass stopper, Apiazon® Type-M high vacuum grease, plastic clips and elastic bands. These samples

Table 1. CASES Expedition Legs, Periods, Location, Number of Stations Visited, and Number of Samples Taken in the Surface Mixed Layer[a]

Leg	Dates	Season	Location	Number of Stations	Number of Samples
1	30 Sep 2003 to 13 Oct 2003	Fall	Mackenzie Shelf and Cape Bathurst Polynya	13	30
2	19 Oct 2003 to 19 Nov 2003	Fall	Mackenzie Shelf, Beaufort Sea and Cape Bathurst Polynya	50	152
7	4–22 Jun 2004	Summer	Cape Bathurst Poylnya	16	76
8	25 Jun 2004 to 1 Aug 2004	Summer	Mackenzie Shelf and Cape Bathurst Polynya	37	162
9	6–10 Aug 2004	Summer	Cape Bathurst Polynya	5	22

[a]Surface mixed layer is 0–30 m.

were kept refrigerated at 4°C until DIC and TA analysis. A third sample was transferred to a 125 mL plastic bottle leaving as small a headspace as possible. The plastic bottles were immersed in a constant temperature bath (25.0 ± 0.05°C) until thermal equilibrium was reached, and the pH was measured within 3 h of collection. Duplicate samples for all three parameters were taken from one depth, usually near but not at the bottom, at every station.

[7] Dissolved inorganic carbon (DIC) concentrations were determined by coulometric titration using a SOMMA instrument [*Johnson et al.*, 1993] fit to a UIC 5011 coulometer. Most analyses were conducted on board, but some from summer 2004 were analyzed ashore within 6 months of collection. Analyses were conducted according to standard protocols [*Dickson and Goyet*, 1994], and the instrument was calibrated against a certified reference material (CRM Batch #61) provided by Andrew Dickson of the Scripps Institute of Oceanography (La Jolla, USA) as well as a secondary standard made from a large quantity of deep water collected early in the expedition, preserved in the same way as the samples, and regularly calibrated directly against CRM Batch #61. Precision, based on the difference between two replicate samples drawn from the same Niskin bottle varied between legs from 2 to 4 μmol kg^{-1}.

[8] Total alkalinity (TA) was measured onboard using an automated Radiometer® (Titrilab 865) potentiometric titrator and a Red Rod® combination pH electrode (pHC2001) in continuous titrant addition mode. Raw titration data were processed with a proprietary algorithm specifically designed for shallow end point detection. The dilute HCl (~0.03N) titrant was calibrated at the beginning and end of each day using certified reference materials (CRM Batch #61) and the secondary standards. Samples were drawn from the sample bottle and dispensed to the open titration vessel with precalibrated water-jacketed, thermostated (25.0 ± 0.05°C) pipettes (~80 mL). The average standard deviation, determined from replicate standard and sample analyses, was 0.3% or 6 μmol kg^{-1}.

[9] The sample pH was determined colorimetrically using a Hewlett-Packard® (HP-8453A) UV visible diode array spectrophotometer and a 5 cm quartz cell. Phenol red (PR) and *m* cresol purple (mCP) were used as indicators and measurements were carried out at the wavelengths of maximum absorbance of the protonated and deprotonated indicators (PR: 433 and 558 nm; mCP: 434 and 578 nm) [*Byrne*, 1987]. A similar procedure was carried out before and after each set of sample measurements using TRIS buffers prepared at a salinity of ~25 and ~35 [*Millero et al.*, 1993]. The salinity dependence of the dissociation constants and molar absorptivities of the indicators were taken from *Robert-Baldo et al.* [1985] for phenol red and from *Clayton and Byrne* [1993] and *Mosley et al.* [2004] for *m* cresol purple. The salinity dependence for the phenol red indicator was extended (from S = 5 to 35) to encompass the range of salinities encountered during this study [*Bellis*, 2002]. All measurements were converted to the total proton scale (pH_t) using the salinity of each sample and the HSO_4^- association constants given by *Dickson* [1990]. Although precisions on the order of 0.0005 pH unit have been reported for spectrophotometric pH measurements [*Clayton and Byrne*, 1993; *Mosley et al.*, 2004], reproducibility and accuracy of our daily TRIS buffer measurements were on the order of 0.005 pH unit or slightly better throughout the 11 month cruise.

[10] As DIC, TA, and pH were measured, the inorganic CO_2 system was overdetermined. The seawater CO_2 fugacity (fCO_2-sw) was calculated from the three possible combinations of measured parameters using CO2SYS [*Lewis and Wallace*, 1998] and the carbonic acid dissociation constants of *Mehrbach et al.* [1973] as refit by *Dickson and Millero* [1987]. Results of our calculations reveal that the in situ pH calculated from DIC and TA was reproduced within 0.04 pH units of the measured value whereas the average standard deviation between measured and calculated DIC (from TA-pH) and TA (from DIC-pH) were 8.4 and 8.5 μmol kg^{-1}, respectively. Finally, the relative standard deviation between the fCO_2-sw calculated from TA-pH and DIC-pH was less than 4 μatm. Many studies dealing with the oceanic carbonate system refer to CO_2 partial pressure (pCO_2) instead of CO_2 fugacity (fCO_2). In fact, both parameters are nearly equal and, at a total pressure of 1 atm, fCO_2 in air is about 0.3% lower than the pCO_2 due to the nonideality of CO_2 [*Weiss*, 1974].

[11] Average fCO_2-sw were computed from 3 to 5 different samples collected within the surface mixed layer (SML). The depth of the SML (usually 0–30 m) is defined as the position of the vertical density gradient maximum at each station. It is important to note that, given the shallow salinity stratification and the strength of external forces (e.g., winds, turbulence), mixing often extends beyond the mixed layer depth (Y. Gratton, personal communication, 2004). The vertical distribution of chemical (e.g., nutrients, TA, DIC, dissolved O_2 concentration) and biological tracers (e.g., Chl *a*) are compatible with this observation. In fact, the calculated fCO_2-sw was often invariant over depths that exceeded the mixed layer depth.

2.2. Meteorological Data Acquisition

[12] A 10 m tower was deployed on the foredeck of the CCGS Amundsen to monitor basic meteorological elements and atmospheric variables relevant to air-sea gas exchange. Horizontal wind speed and direction were measured at a height of 14.6 m above the sea surface, using a wind monitor

(RM Young Co.®, model 15106MA). Temperature and relative humidity were measured using a relative humidity-temperature probe (Vaisala®, model HMP45C212) housed in a vented sunshield. Atmospheric pressure was measured approximately 6.5 m above the sea surface using a Vaisala barometric pressure sensor (model PTB101B). Incoming short-wave and long-wave radiation were measured using a gimbaled pyranometer and pyrgeometer, respectively (Eppley Laboratory, Inc. model PSP, and PIR). Measurements were taken every three seconds by these instruments and recorded as 1 min averages on a data logger (Campbell Scientific Inc. model CR-23X). True wind speed and direction were computed during post processing using ship navigation data. The NOAA/COARE v3.0 algorithm [*Fairall et al.*, 2003] was used to compute atmospheric stability parameters to correct wind speed to 10 m above the sea surface following *Stull* [1988]. Data ingested into the NOAA/COARE algorithm included hourly averages of true wind speed at measurement height, air temperature, humidity and radiation, in conjunction with the average seawater temperature within the upper 5 m from the closest CTD cast in both time and space. Periods where wind direction exceeded ±100° from the ship's bow were removed from subsequent analyses.

2.3. Computation of Air-Sea CO_2 Fluxes

[13] Air-sea CO_2 fluxes were first computed assuming ice-free conditions and using the bulk flux equation: $FCO_2 = k_s S(fCO_2sw - fCO_2atm)$, where FCO_2 is the flux of CO_2 (mmol m^{-2} d^{-1}, negative values indicate a sink into the ocean while positive values indicate a source for the atmosphere), fCO_2 is the fugacity of CO_2 (μatm) in seawater (sw) and atmosphere (atm), k_s is the gas transfer velocity (cm h^{-1}), S is the CO_2 solubility (mol m^{-3} atm^{-1}), which was calculated using sea surface temperature and salinity and the equations of *Weiss* [1974]. Atmospheric fCO_2 was calculated using atmospheric CO_2 mixing ratio data from Point Barrow in Alaska [*Keeling et al.*, 2008], using in situ sea surface temperature, salinity, barometric pressure, and the expressions of *Weiss* [1974] and *Weiss and Price* [1980]. The hourly CO_2 mixing ratio data were downloaded from http://www.cmdl.noaa.gov (National Oceanographic and Atmospheric Administration, NOAA, Climate and Meteorological Diagnostics Laboratory, CMDL). The meteorological data were matched to the closest near surface fCO_2-sw measurements within 1 day of the fCO_2-atm. Hourly transfer velocity (k_s) was calculated using the algorithm of *Sweeney et al.* [2007]: $k_s = 0.27U_{10m}^2(Sc/660)^{1/2}$, where U_{10m} is the 10 m wind speed and Sc is the Schmidt number of CO_2 [*Jähne et al.*, 1987].

[14] Numerous relationships have been developed between k_s and 10 m winds, and yet k_s remains the largest single source of uncertainty in flux calculations, particularly at high wind speeds (>10 ms^{-1}). The impact of different gas exchange formulations and wind speed on global air-sea CO_2 fluxes has been recently reviewed by *Wanninkhof* [2007]. The review concludes that the global fluxes are very sensitive to estimates of gas transfer rate and the parameterization of gas transfer with wind. Parameterizations of gas exchange with wind differ in functional form and magnitude but the difference between the most used quadratic relationships is about 15%. Based on current estimates of uncertainty of the air-sear fCO_2 differences, the winds, and the gas exchange-wind speed parameterization, each parameter contributes similarly to the overall uncertainty in the flux that is estimated at 25%. The *Sweeney et al.* [2007] parameterization used in this study is based on a global inventory of bomb-produced radiocarbon in the oceans and, importantly, compares exceptionally well with direct measurements of k_s at low to moderate [*McGillis et al.*, 2001] as well as at high wind speeds [*Ho et al.*, 2006]. We undertook separate flux calculations using other commonly used transfer velocity formulations (including *Wanninkhof* [1992], *Liss and Merlivat* [1986], and *Wanninkhof and McGillis* [1999]) to facilitate comparisons with other studies. However, the uncertainty associated with the application of the bulk parameterization has not been defined in marginal ice environments and this remains a subject of inquiry.

[15] The computed air-sea CO_2 fluxes, that assume ice-free conditions, were then scaled using a multiplier equal to 100% minus the % ice coverage. It is assumed here that sea ice provides an effective barrier to air-sea CO_2 gas exchange, and that air-sea CO_2 fluxes are a linear function of sea ice coverage. At 100% ice coverage, we set the multiplier to 1% for consistency with previous studies [*Bates*, 2006]. Sea ice concentration in proximity to the ship was estimated from the National Snow and Ice Data Center's (NSIDC) AMSR-E ice concentration archive [*Cavalieri et al.*, 2004]. The AMSR-E ice concentration from the nearest pixel to each CTD station was used in the analysis. Pixel resolution is 12.25 km and the accuracy of the classification is about 7% [*Steffen et al.*, 1992], but can easily increase to 27–43% in seasonal ice zones where thin ice or mixed water/ice pixels predominate [*Comiso et al.*, 1997; *Agnew and Howell*, 2003]. We note that sea ice is not actually impermeable to gases [*Gosink et al.*, 1976; *Semiletov et al.*, 2004; *Zemmelink et al.*, 2006; *Loose et al.*, 2009], but the mechanisms by which CO_2 exchanges with sea ice are very different from direct air-sea gas exchange and have not yet been parameterized. Therefore, we have not included the effects of air-ice or ice-water CO_2 transfer in this study of direct air-sea CO_2 exchange. The air-sea CO_2 flux that takes into account the ice cover is indicated by FCO_2-ic.

3. Results

3.1. Distributions of Sea Surface Temperature, Salinity, and Chlorophyll *a*

[16] Our data set was separated into two time periods, the fall of 2003 (late September to mid-November, 2003) and the summer of 2004 (June–August 2004). Figure 2 shows the spatial distributions of sea surface temperature (SST), salinity, and Chl *a* for both periods. In fall 2003, the SST was close to the freezing point at all stations with values ranging from −1.5 to −0.4°C. Surface waters with relatively low salinity (<22) were found along the Kugmalitt Trough while higher salinities (>28) were observed in the southeastern Beaufort Sea and the Cape Bathurst Polynya. The summer 2004 period was characterized by an increase in the Mackenzie River discharge and accompanied by a very low sea surface salinity (8.8) and SST as high as 10.3°C along the Mackenzie Trough. The influence of the Mackenzie plume was therefore limited to the western part of the shelf, at least at the time of our observations. Offshore, SST

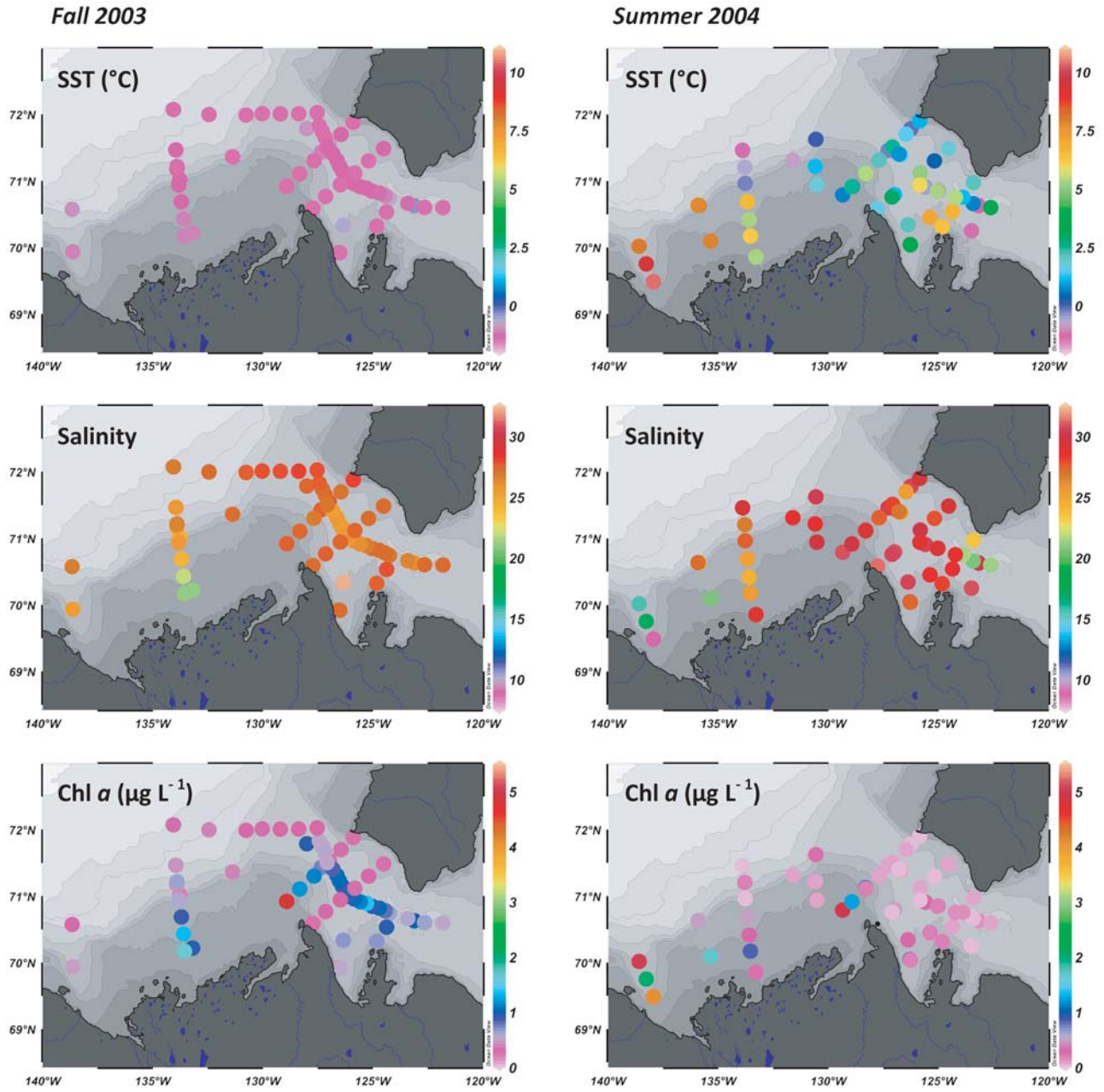

Figure 2. Spatial distribution of sea surface temperature (SST, in °C), salinity, and chlorophyll *a* concentration (Chl *a*, in μg L^{-1}) recorded in fall 2003 and summer 2004.

decreased to −1.3°C while surface salinity increased to 29 in the Beaufort Sea. Higher salinities (>30) were observed in the Cape Bathurst Polynya and lower values (<24) were measured in the Amundsen Gulf, probably due to sea ice melt. Surface Chl *a* distributions, derived from fluorescence measurements, show relatively high Chl *a* concentrations (>4 μg L^{-1}) in the vicinity of Cape Bathurst in fall and summer and along the Mackenzie Trough in summer. In contrast, all other stations of the study area display very low Chl *a* concentrations (<1 μg L^{-1}), at least in surface water.

3.2. Variability of the Carbonate System Parameters

[17] The distribution patterns of the carbonate parameters (DIC, TA, pH_t and fCO_2-sw) in the SML were very different between the two study periods (Figure 3). In fall 2003, relatively small spatial variations in the carbonate parameters were observed at stations visited during this season. If we average all measurements (±standard deviation) made in the SML over this period, DIC and TA were 1910 ± 50 μmol kg^{-1} and 2000 ± 60 μmol kg^{-1}, respectively, with the lowest values observed on the Mackenzie Shelf and the highest in the Cape Bathurst Polynya. Similarly, average pH_t was nearly constant at 8.13 ± 0.03 over the whole study area. Values of fCO_2-sw ranged from 238 to 321 μatm with an average fCO_2-sw of 287 ± 18 μatm over the study area (Table 2). In contrast, the carbonate parameters were more variable among stations in summer 2004, especially off the Mackenzie River mouth and at Cape Bathurst, in response to

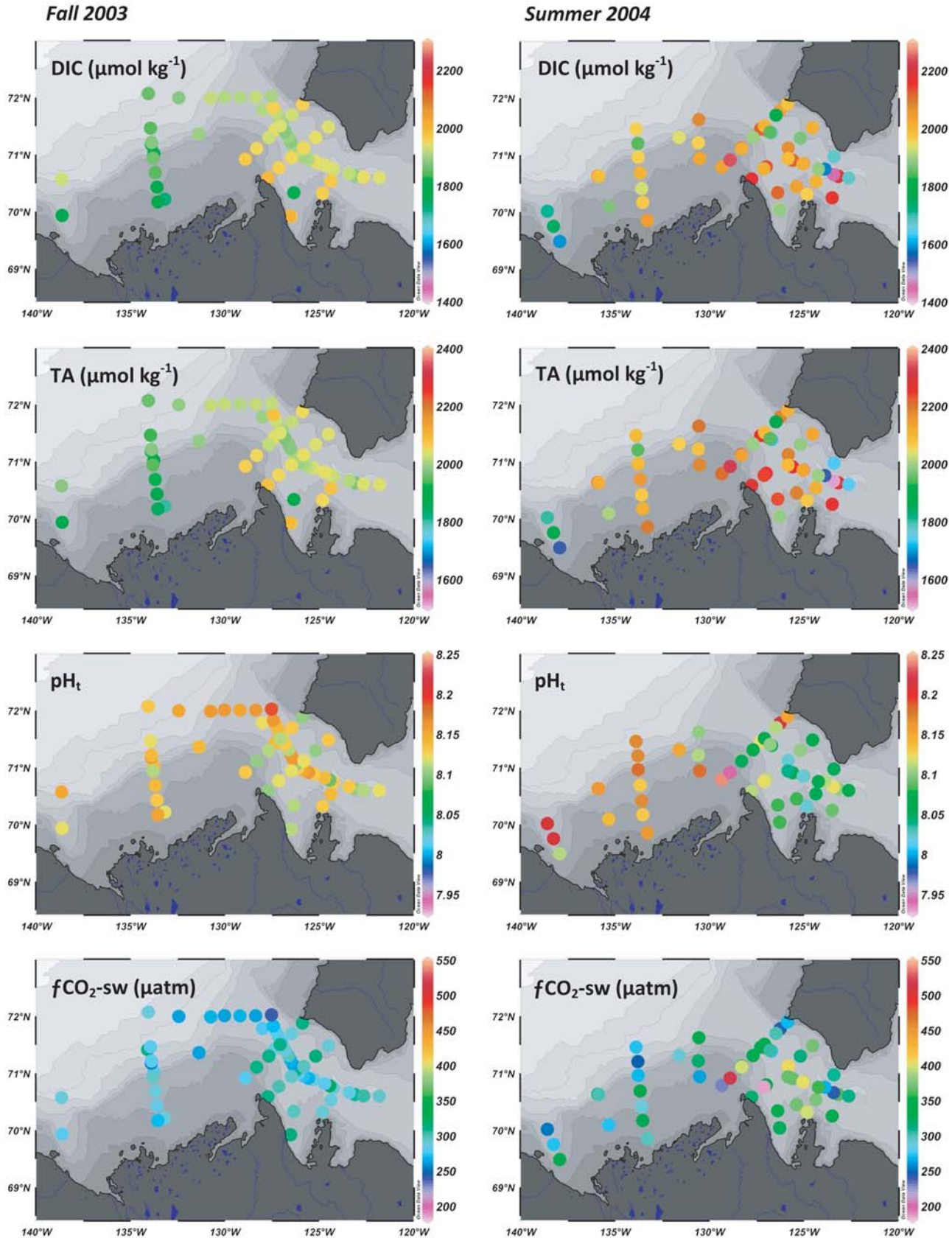

Figure 3. Spatial distribution of dissolved inorganic carbon (DIC, in μmol kg^{-1}), total alkalinity (TA, in μmol kg^{-1}), pH_t, and CO_2 fugacity (fCO_2-sw, in μatm) in the surface mixed layer for fall 2003 and summer 2004.

Table 2. Averages fCO_2-sw in the Surface Mixed Layer for the Three Physiographic Regions[a]

Region	Fall 2003		Summer 2004		
	fCO_2-sw	Number of Samples	fCO_2-sw	Number of Samples	Average fCO_2-sw
Beaufort Sea	273 ± 13	29	288 ± 33	24	280 ± 25
Mackenzie Shelf	293 ± 21	31	326 ± 65	62	315 ± 57
Cape Bathurst Polynya	290 ± 16	84	341 ± 44	113	319 ± 43
Average	287 ± 18		330 ± 53		312 ± 47

[a]Averages fCO_2-sw are given in μatm with ± standard deviation.

freshwater input and upwelling event, respectively. The fCO_2-sw distribution was more heterogeneous in summer 2004 than in the fall 2003 with an average fCO_2-sw of 330 ± 53 μatm. The lowest and highest fCO_2-sw values (184 and 515 μatm, respectively) were both recorded at Cape Bathurst, indicating a strong small-scale variability in this region.

3.3. Water Mass Properties

[18] In the study area, the surface water properties vary seasonally because of freshwater discharge, sea ice formation/melting and other factors such as vertical mixing and primary production. Indeed, T-S diagrams show very different properties in surface water masses from fall to summer conditions (Figure 4). As described by *Macdonald et al.* [1989], the SML of the southeastern Beaufort Sea is a mixture of 3 main water masses: Mackenzie River water (MW), polar mixed layer (PML), and sea ice melt (SIM). Below the SML, the upper halocline water is characterized by salinity of 33.1 (around 150 m depth) and this water mass is derived from the Pacific Water (PW). Pacific water enters the Canada Basin via the Bering Strait and is seasonally modified in the Chukchi Sea by heat exchange, ice formation and melting, biological production and interaction with the sediment [*Macdonald et al.*, 2002; *Pickart*, 2004; *Woodgate et al.*, 2005]. Water from the Pacific is known to be nutrient rich and DIC rich and therefore supersaturated (fCO_2-sw > 550 μatm) with respect to atmospheric CO_2 [*Pipko et al.*, 2002; *Loeng et al.*, 2005; *Semiletov et al.*, 2007].

3.4. Air to Sea CO_2 Fluxes

[19] The direction and magnitude of the air-sea CO_2 fluxes are mainly driven by the fCO_2 gradient between the seawater and the overlying atmosphere, the ice cover, and the wind stress that accelerates gas exchange. During the CASES expedition, the ice cover ranged from 84 to 100% in fall 2003 and from 0 to 66% in summer 2004, depending on location and date (Table 3 and Figure 5). The wind speed was also highly variable and periods of weak (<4 m s^{-1}) and strong (>10 m s^{-1}) winds were recorded during both seasons. However, the average wind speed was slightly higher in fall 2003 (6.2 ± 2.6 m s^{-1}) than in summer 2004 (5.5 ± 2.2 m s^{-1}). The air-sea CO_2 fluxes were first computed assuming ice-free conditions (FCO_2). Due to lower SML fCO_2-sw, the potential uptake of atmospheric CO_2 by the ocean was higher in fall 2003 than in summer 2004 with average FCO_2 of -11.1 ± 9.7 mmol m^{-2} d^{-1} and −4.8 ± 5.4 mmol m^{-2} d^{-1}, respectively (Table 3).

[20] However, air-sea CO_2 fluxes are greatly limited by sea ice cover even if the exchange of CO_2 at the air-ice-sea interface cannot be ignored. When sea ice cover reaches 100%, it is possible that air-sea CO_2 gas exchange can occur through leads and fractures in the ice, and also directly through sea ice [*Semiletov et al.*, 2004]. In this study, FCO_2-ic was computed with a reducing factor to account for ice cover and we used the same factor as *Bates* [2006]. The reducing factor assumes that air-sea CO_2 gas exchange is inversely proportional to ice cover and only 1% of the flux could pass through at >99% sea ice coverage. In fall 2003, FCO_2-ic

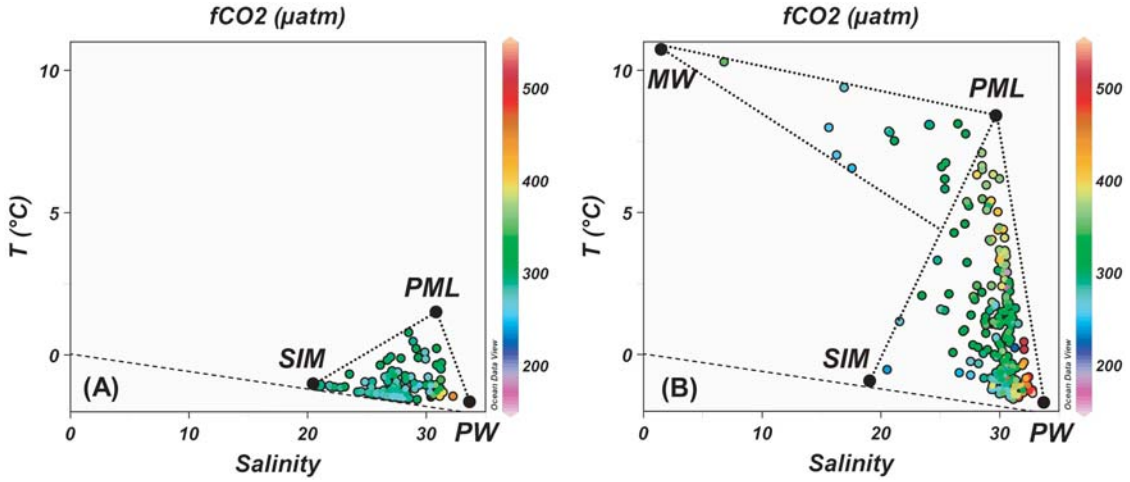

Figure 4. Temperature and salinity diagram with fCO_2-sw (in μatm) for the surface mixed layer (0–30 m) of the southeastern Beaufort Sea during (a) fall 2003 and (b) summer 2004. The dashed line shows the freezing point at the given temperature and salinity. Source water types are also indicated as follow: MW, Mackenzie River water; SIM, sea ice melt; PML, polar mixed layer; PW, Pacific water.

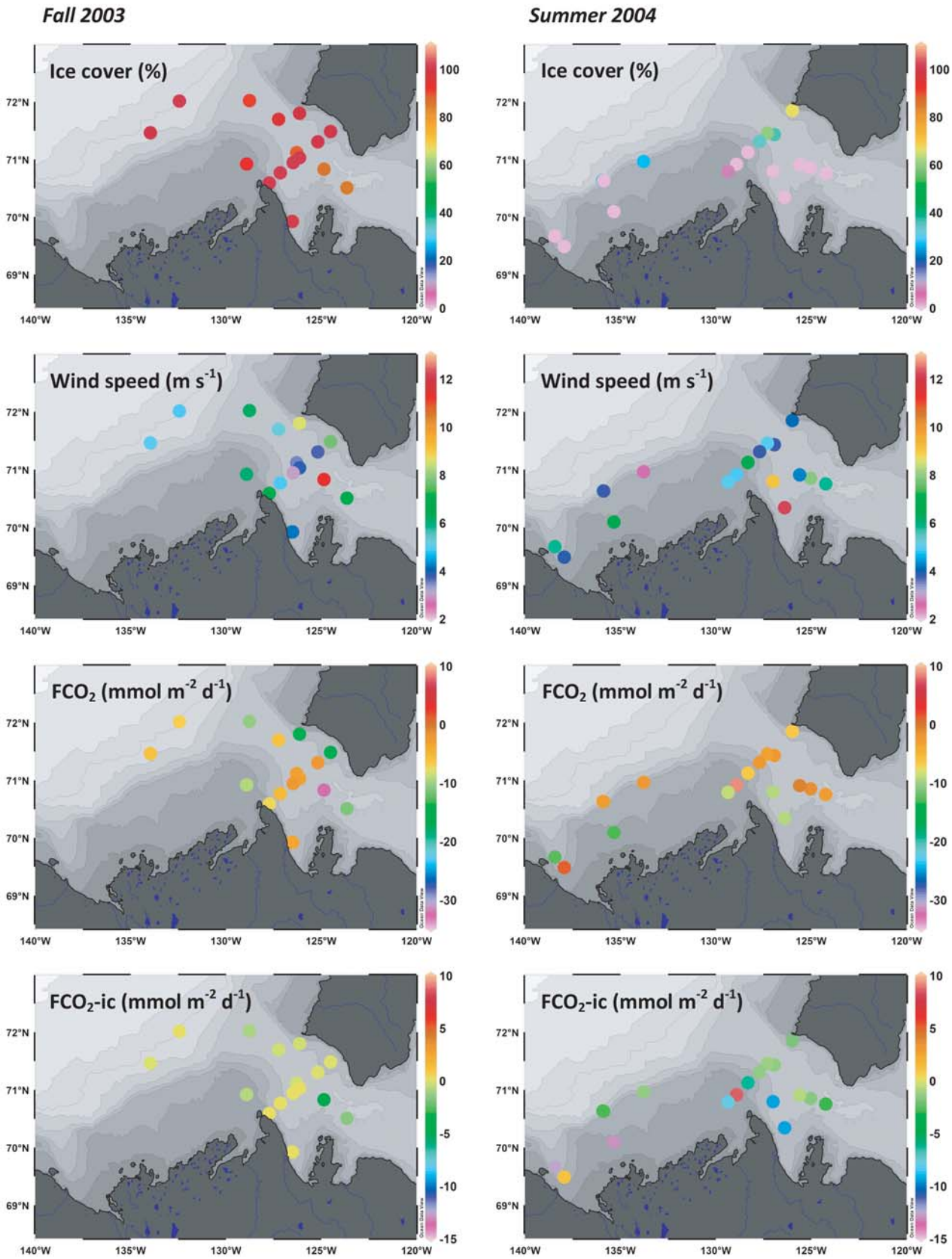

Figure 5. Distributions of ice cover (in %), wind speed (in m s^{-1}), and air-sea CO_2 flux (in mmol m^{-2} d^{-1}) for fall 2003 and summer 2004. The CO_2 fluxes were computed from atmospheric and surface mixed layer fCO_2, as well as from hourly-averaged meteorological data and assuming either ice-free conditions (FCO_2) or using a reducing factor that accounts for the ice cover (FCO_2-ic; see text for details).

Table 3. Averages, Standard Deviations, and Minima and Maxima of Ice Cover, Wind Speed, and Computed Air-Sea CO_2 Fluxes Assuming Ice-Free Conditions and Taking Into Account the Ice Cover for Fall 2003 and Summer 2004[a]

	Period	Average	σ	Minimum	Maximum
Ice cover (%)	Fall 2003	92	6	84	100
	Summer 2004	14	22	0	66
Wind speed (m s^{-1})	Fall 2003	6.2	2.6	3.0	11.4
	Summer 2004	5.5	2.2	2.7	12.2
FCO_2 (mmol m^{-2} d^{-1})	Fall 2003	−11.1	9.7	−32.4	−2.1
	Summer 2004	−4.8	5.4	−13.1	+8.6
FCO_2-ic (mmol m^{-2} d^{-1})	Fall 2003	−1.2	1.7	−4.9	−0.1
	Summer 2004	−4.3	5.5	−13.1	+8.6

[a]Here σ is the standard deviation and FCO_2 and FCO_2-ic are computed air-sea CO_2 fluxes assuming ice-free conditions and taking into account the ice cover, respectively.

ranged from −4.9 mmol m^{-2} d^{-1} in relatively open water of the Cape Bathurst Polynya to −0.1 mmol m^{-2} d^{-1} in the southeastern Beaufort Sea. The presence of multiyear ice in the Beaufort Sea greatly restricts the CO_2 uptake rate by the ocean. Unfortunately, FCO_2-ic were not computed for the western Mackenzie Shelf in fall 2003 because meteorological data are missing. However, the SML was undersaturated with respect to atmospheric CO_2, suggesting that the Mackenzie Shelf is a sink of CO_2 at this period. In summer 2004, the Mackenzie Shelf was free of ice and FCO_2-ic ranged from −13.1 mmol m^{-2} d^{-1} on the western part of the shelf to +8.6 mmol m^{-2} d^{-1} on the eastern part, i.e., close to the Cape Bathurst upwelling region.

4. Discussion

[21] High temporal and spatial variability in seawater properties are expected in Arctic river-dominated ocean margins as a result of freshwater discharge and sea ice cycle. Hence, the seawater carbonate system is poorly constrained and, because of a lack of data, the direction and magnitude of air-sea CO_2 fluxes in the Arctic Ocean are poorly known. The CASES data set provides a unique opportunity to assess these in the Beaufort Sea and establish a baseline for future studies with respect to potential climate change feedback. The CASES data set extends throughout the water column, but in this paper we focus on surface processes that affect the CO_2 fluxes at the air-sea interface. A preliminary examination of the data reveals that surface mixed layer fCO_2-sw in the southeastern Beaufort Sea varied little over the period of observation, whereas large variations of all measured carbonate parameters were observed on the Mackenzie Shelf and in the Cape Bathurst Polynya. In order to discuss the temporal and spatial variability, we divided the study area into the following four physiographic regions: (1) the southeastern Beaufort Sea with the presence of multiyear ice; (2) the western part of the Mackenzie Shelf that is prone to seasonal inputs of freshwater by the Mackenzie River; (3) the eastern part of the Mackenzie Shelf, including Cape Bathurst, which is a recognize site for upwelling event; and (4) the Cape Bathurst Polynya with recurrent open water and warm SST in summer.

4.1. Southeastern Beaufort Sea

[22] During the CASES expedition, only the southeastern part of the Beaufort Sea was investigated because of the presence of multiyear ice. The SML of the Beaufort Sea was mostly a mix of SIM and PML in both seasons, as indicated by the T-S diagrams. The DIC-rich water of the upper halocline (PW) remains below the SML due to strong thermohaline stratification. In fall 2003, fCO_2-sw values were nearly constant at 273 ± 13 μatm (Table 2) and the SML was always undersaturated with respect to atmospheric CO_2 (378 μatm). Assuming ice-free conditions, we computed an average FCO_2 of −7.8 ± 2.8 mmol m^{-2} d^{-1} for the southeastern Beaufort Sea. But at that time, the ice cover was close to 100% and therefore the FCO_2 values were not realistic. Then, we included a reduction factor for the ice cover and we computed an average FCO_2-ic of −0.5 ±

Table 4. Comparison of Air-Sea CO_2 Fluxes With Other Arctic Zones

Region	Period	Air-Sea CO_2 Fluxes (mmol m^{-2} d^{-1})	Parameterization Used for CO_2 Transfer Velocity[a] (k_s)	Reference
Beaufort Sea	Fall 2003	−5.8	LM86	This study
Beaufort Sea	Summer 2004	−3.2	LM86	This study
Beaufort Sea	Fall 2003	−9.9	W92	This study
Beaufort Sea	Summer 2004	−5.7	W92	This study
Beaufort Sea	Fall 2003	−9.0	WM99	This study
Beaufort Sea	Summer 2004	−4.7	WM99	This study
Beaufort Sea	Fall 2003	−9.1	S07	This study
Beaufort Sea	Summer 2004	−5.2	S07	This study
Beaufort Sea	Summer 1998–2000	−12.0	WM99	[*Murata and Takizawa*, 2003]
Mackenzie Shelf	Summer 2005	−6.0	W92	[*Fransson et al.*, 2009]
Chukchi Sea	Fall 1996	−14.6 ± 13.1	W92	[*Pipko et al.*, 2002]
Chukchi Sea	Fall 1996	−10.2 ± 10.1	WM99	[*Pipko et al.*, 2002]
Chukchi Sea	Summer-fall 2000	−7.7 ± 8.3	W92	[*Semiletov et al.*, 2007]
Chukchi Sea	Summer-fall 2002	−17.0 ± 12.7	W92	[*Semiletov et al.*, 2007]
Chukchi Sea	Spring-summer 2002	−40.0 ± 10.0	W92	[*Bates*, 2006]
East Siberian Sea	Fall 2003	+1.0 ± 1.6	W92	[*Semiletov et al.*, 2007]
East Siberian Sea	Fall 2004	+10.9 ± 12.6	W92	[*Semiletov et al.*, 2007]
Laptev Sea	Fall 2005	−1.2 to +1.7	W92	[*Semiletov et al.*, 2007]
Barents Sea	Summer 1999	−9.5	W92	[*Kaltin et al.*, 2002]
Baffin Bay	Year-round 1998–1999	−1.0	LM86	[*Miller et al.*, 2002]
Hudson Bay	Fall 2005	−0.7	S07	[*Else et al.*, 2008]
Greenland Sea	Year-round 1993–1997	−12.1 ± 0.9	W92	[*Anderson et al.*, 2000]

[a]W92 is *Wanninkhof* [1992], LM86 is *Liss and Merlivat* [1986], and WM99 is *Wanninkhof and McGillis* [1999].

0.5 mmol m^{-2} d^{-1}. Because of sea ice retreat, the CO_2 uptake rate was slightly larger in summer 2004, with FCO_2-ic ranging from −2.8 to −1.5 mmol m^{-2} d^{-1}, despite the smaller air-sea fCO_2 gradient and wind stress. The SML remained undersaturated (288 ± 33 μatm) and primary production appeared to contribute little to the surface water fCO_2 drawdown (very low Chl *a* concentrations). Indeed, there was no significant relationship between surface Chl *a* concentration and fCO_2-sw. In summer, the deep chlorophyll maximum is usually located below the SML, around 30 to 50 m depth, due to nutrient depletion in the SML [*Carmack et al.*, 2004]. This implies that biological production was minor as a possible cause of the variations in surface water fCO_2, at least at the time of our observations.

[23] Although variable, the computed CO_2 fluxes (uncorrected for ice cover) are lower than those reported in previous studies of the Beaufort Sea but usually in agreement with other Arctic regions (Table 4). In fact, the direction and magnitude of air-sea CO_2 fluxes demonstrate a strong variability in both space and time. Air-sea CO_2 fluxes range from strong negative value (−40.0 ± 10.0 mmol m^{-2} d^{-1}) in the Chukchi Sea, due to high rates of localized primary production [*Bates*, 2006], to strong positive value (+10.9 ± 12.6 mmol m^{-2} d^{-1}) in the East Siberian Sea, because of oxidation of terrestrial organic matter [*Semiletov et al.*, 2007]. Since the time and space scales differ among the studies, direct comparison with our results is difficult. However, the summer FCO_2 value for the southeastern Beaufort Sea is lower than the FCO_2 reported by *Murata and Takizawa* [2003] for the western Beaufort Sea (−12 mmol m^{-2} d^{-1}). Irrespective of sea ice cover, the Beaufort Sea is a small to moderate annual CO_2 sink.

4.2. Western Mackenzie Shelf Influenced by Freshwater Inputs

[24] The spread of the Mackenzie River plume on the continental shelf is highly constrained by runoff and air temperature that play an obvious role in the sea ice freeze/melt cycle [*Carmack and Macdonald*, 2002]. During our study, the influence of the Mackenzie River on the shelf water chemistry was limited to the inner continental shelf, as demonstrated by SST and salinity gradients. Our results (Figures 2 and 3) reveal that the low salinity ($21 < S < 28$) and cold surface waters ($-1.5°C < t < -0.9°C$) sampled on the western Mackenzie Shelf in the fall of 2003 were undersaturated (270 μatm < fCO_2-sw < 290 μatm) with respect to the overlying atmosphere (378 μatm). Hence, this part of the Mackenzie Shelf probably acted as a sink for atmospheric CO_2 in the fall even though, in the absence of meteorological data, we could not compute the FCO_2 for that period. Similarly, the low salinity ($8.8 < S < 32$) but warmer waters ($-1.5°C < t < 10.3°C$), sampled on the Mackenzie Shelf soon after the ice breakup and throughout the summer of 2004, were also mostly undersaturated (230 μatm < fCO_2-sw < 350 μatm) with respect to the atmosphere. Very few fCO_2 data from the Mackenzie River are available in the literature, but *Vallières et al.* [2008] reported fCO_2 supersaturation in the Mackenzie River with values as high as 690 μatm in late July 2004. Such high fCO_2 values were not observed off the Mackenzie River mouth during our study and the highest fCO_2-sw value that we measured on the western part of the shelf was 350 μatm.

[25] The relatively low fCO_2-sw observed off the Mackenzie River is certainly the result of water mixing, decreasing temperature and enhanced primary production. At the Mackenzie River mouth, the warm freshwater (+15°C) forms a thin plume over the colder (−1°C) polar mixed layer below. Despite the strong density gradient, the Mackenzie River water and the PML should mix rapidly to produce the large offshore variations observed in all parameters. The number of data along the salinity gradient is too small to determine an empirical temperature dependence of fCO_2-sw. However, if we assume the thermodynamic relationship for cold water (9.9 μatm °C) given by *Takahashi et al.* [1993], a decrease in SST by 16°C results in a fCO_2-sw change of −160 μatm. Therefore, vertical mixing and temperature variations play an obvious role in decreasing the fCO_2-sw in front of the Mackenzie River mouth. At the same time, relatively high Chl *a* concentrations (>4 μg L^{-1}) were observed along the Mackenzie Trough, in concomitance with low fCO_2-sw (253 μatm). The DIC uptake by the biological production is a possible cause of the low surface water fCO_2-sw but there was no significant relationship between Chl *a* and fCO_2-sw. The increase in primary production off the Mackenzie River mouth results not so much from an increase in light availability but rather from an increased nutrient supply through river runoff, wind mixing and shelf break upwelling [*Carmack et al.*, 2004]. Hence, the horizontal fCO_2-sw gradient through the Mackenzie delta was controlled by vertical mixing, temperature variations and possibly primary production. The evaluation of the relative contributions of each parameter to the offshore decreasing fCO_2-sw requires more data along the Mackenzie River delta and further examination.

[26] The highest negative FCO_2-ic values (−13.1 mmol m^{-2} d^{-1}) were recorded in summer 2004 on the Mackenzie Shelf and along the Mackenzie Trough. The average summer FCO_2-ic was −6.3 ± 6.0 mmol m^{-2} d^{-1}, which is close to the FCO_2 value reported by *Fransson et al.* [2009] for the Mackenzie Shelf (−6.0 mmol m^{-2} d^{-1}). However, the FCO_2-ic varies along the Mackenzie Shelf form strong negative values to strong positive values (+8.5 mmol m^{-2} d^{-1}) observed on the eastern Mackenzie Shelf at Cape Bathurst. These large variations are related to vertical mixing and intermittent upwelling that occur on the Mackenzie Shelf. In Fact, the shelf is cut at its southwestern end by the Mackenzie Trough, in the middle by the narrow and shallow Kugmallit Trough (immediately north of the Mackenzie delta), and at its northeastern end by the steep slope into Amundsen Gulf at Cape Bathurst (Figure 1). All are recognized sites of topographically enhanced upwelling during times of southwestward surface stress from wind or ice motion [*Carmack and Kulikov*, 1998; *Williams et al.*, 2006, 2008]. As demonstrated by *Kulikov et al.* [2004], strong barotropic and baroclinic tidal currents occur in that area, which may induce important vertical mixing on the northeastern Mackenzie Shelf.

4.3. Effects of Upwelling on the Eastern Mackenzie Shelf

[27] A six-station transect along the eastern part of the Mackenzie Shelf clearly shows evidence of an upwelling event at Cape Bathurst. Figure 6 shows the vertical distribution of temperature, salinity, Chl *a*, DIC and fCO_2-sw along this transect from 17 to 21 June 2004 (CASES, Leg 7).

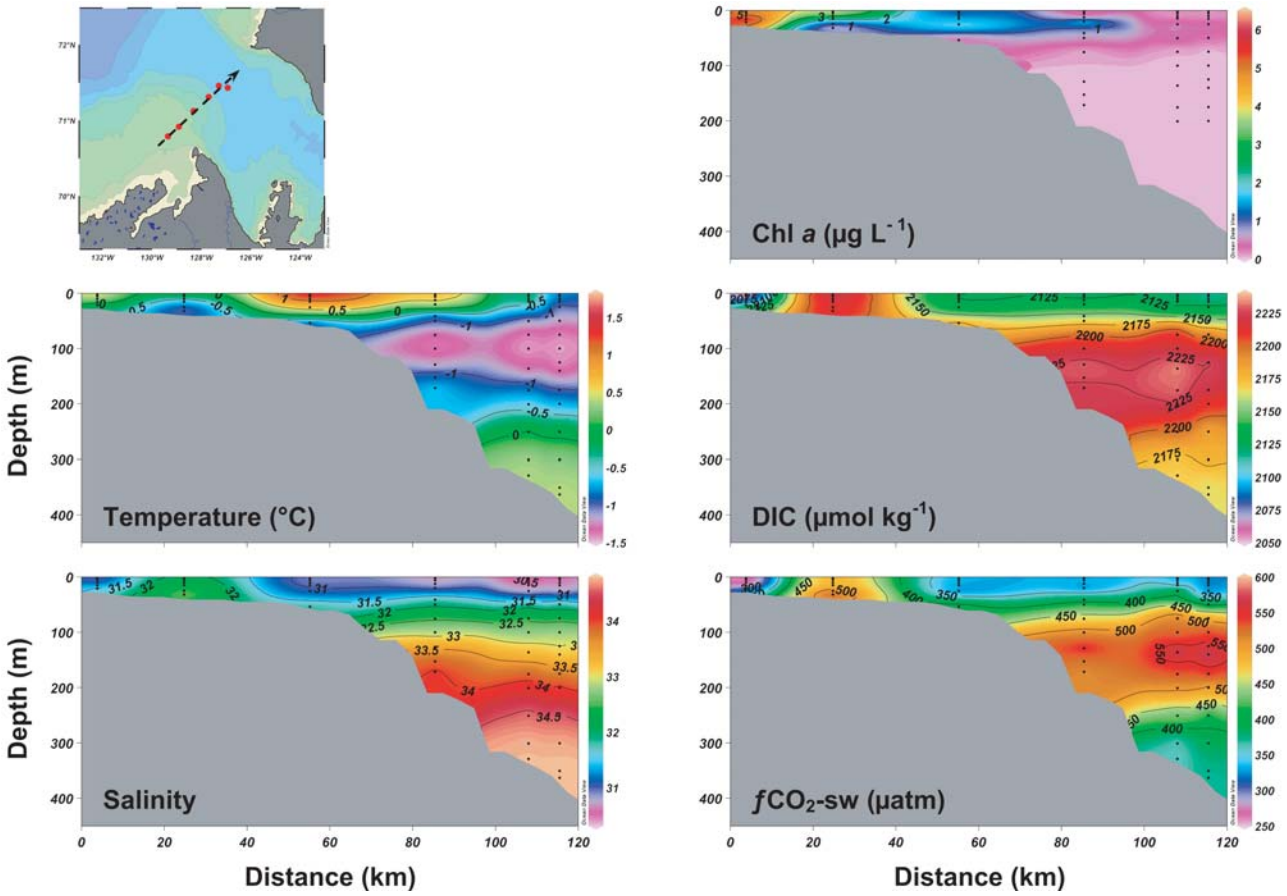

Figure 6. Vertical distribution of temperature (in °C), salinity, Chl *a* (in μg L^{-1}), DIC (in μmol kg^{-1}), and fCO_2-sw (in μatm) along a SW-NE six-station transect from the eastern part of the Mackenzie Shelf to the Cape Bathurst Polynya (data collected from 17 to 21 June 2004).

The SML in the Cape Bathurst Polynya (distance > 50 km on Figure 6) was characterized by a relatively low salinity (30.7 ± 0.2), low DIC concentration (2120 ± 8 μmol kg^{-1}), and low Chl *a* concentration (0.6 ± 0.7 μg L^{-1}). As a result, the fCO_2-sw were relatively low (320 ± 12 μatm), indicating that the SML was undersaturated with respect to the atmosphere. On the other hand, the station located on the Mackenzie Shelf, close to Cape Bathurst (distance = 25 km on Figure 6), displays a concomitant increase of salinity (32.4 ± 0.4), DIC (2232 ± 7 μmol kg^{-1}) and very high fCO_2-sw (522 ± 37 μatm) in the SML. These observations are consistent with the upwelling of Pacific derived upper halocline water on the Mackenzie Shelf. Indeed, the upper halocline is characterized by a salinity of 33.1, high DIC concentration (>2200 μmol kg^{-1}), and fCO_2-sw up to 550 μatm [*Pipko et al.*, 2002; *Semiletov et al.*, 2007]. The T-S diagram for summer 2004 also supports the fact that very high fCO_2-sw in the SML is related to the upwelling of Pacific water (Figure 4). The Pacific water is nutrient rich and its upwelling on the Mackenzie Shelf should stimulate primary productivity when enough light is available [*Tremblay et al.*, 2008]. At the time of sampling, the increase of Chl *a* concentration (>4 μg L^{-1}) in the first 10 m of the water column was apparently not strong enough to counteract the high level of fCO_2-sw. Conversely, at the shallowest Mackenzie Shelf station (distance = 5 km on Figure 6), very low levels of fCO_2-sw (230 ± 7 μatm) are observed. The strong dropoff in fCO_2-sw over a relatively short distance (less than 20 km) is interpreted as an increase in primary production, as revealed by relatively high Chl *a* concentrations of 5.3 ± 0.6 μg L^{-1}. This example illustrates the high spatial variability in fCO_2-sw on the Mackenzie Shelf due to the complex interplay of physical and biological processes. Our results, based on carbonate parameters and computed fCO_2-sw, clearly highlight the upwelling of Pacific CO_2-rich water on the shelf at Cape Bathurst.

4.4. Cape Bathurst Polynya

[28] The Cape Bathurst Polynya is a direct consequence of the Beaufort Sea gyre and a series of flaw leads creating conditions conducive to oceanic upwelling [*Barber and Hanesiak*, 2004]. Although the Cape Bathurst Polynya exhibits marked interannual variability in the timing of sea ice retreat and formation, the ice-free period usually starts in June and first year ice forms during October, resulting in an average 4 month open water season. In fall 2003, FCO_2-ic ranged from −4.7 to −0.1 mmol m^{-2} d^{-1}, and the Cape Bathurst Polynya served as a small to moderate sink for atmospheric CO_2. In summer 2004, CO_2 fluxes across the air-sea interface were highly variable and ranged from −9.4 to −0.8 mmol m^{-2} d^{-1}, indicating that the polynya could act as a weak to strong sink of CO_2, depending on station location

and date. Seasonal variations of SST are marked in the polynya and have a strong influence on the fCO_2-sw. In fall 2003, the average fCO_2-sw in the cold SML (-1.12 ± 0.52°C) of the Cape Bathurst Polynya was 290 ± 16 μatm. By the summer of 2004, the SST in the Cape Bathurst Polynya had increased to $+3.4 \pm 2.2$°C and average fCO_2-sw reached 341 ± 44 μatm. According to the thermodynamic dependence of temperature and fCO_2-sw [*Takahashi et al.*, 1993], an increase of SST by 5°C results in a fCO_2-sw change of +50 μatm. This calculation is in good agreement with our observations. Therefore, variation in temperature can explain almost all of the fCO_2-sw seasonal variation observed in the Cape Bathurst Polynya.

[29] The ice-free period is favorable for upwelling of deep and nutrient-rich waters that sustain a relatively high primary production. Phytoplankton blooms occur mainly in June and in September, associated with Chl *a* concentrations of 2 to 8 μg L^{-1} [*Arrigo and van Dijken*, 2004; *Tremblay et al.*, 2008]. During our period of observation, surface Chl *a* concentrations were relatively low (<1 μg L^{-1}) in the Cape Bathurst Polynya and the Chl *a* concentrations were slightly higher in fall 2003 than in summer 2004. In summer, the deep chlorophyll maximum is usually located below the SML and close to the nutrient-rich water. In fall, vertical mixing and upwelling event bring nutrient-rich water close to the surface and can increase the primary production. Again, there was no relationship between Chl *a* and fCO_2-sw. The biological production seems to have a little effect on the fCO_2-sw, but this topic needs further examination.

5. Conclusion

[30] Understanding the link between ocean physics and the biogeochemistry of the carbonate system is a first step in predicting the response of the Arctic system to climate change. One of the most conspicuous effects of climate change in the Arctic Ocean is the decrease of ice cover which has been strikingly large in the southeastern Beaufort Sea [*Barber and Hanesiak*, 2004]. Some authors argue that the loss of ice cover on the Arctic continental margins will increase the magnitude of the CO_2 sink in the Arctic Ocean [*Anderson and Kaltin*, 2001; *Bates*, 2006]. However, this statement should be tempered because many factors could decrease the CO_2 sink. For example, increased precipitation and consequent amplified river discharge is expected to result in a greater export of terrigenous carbon, both in dissolved (DOC) and particulate (POC) form, to the Arctic Ocean [*Benner et al.*, 2004]. Warming will induce thawing of the permafrost [*Goulden et al.*, 1998] and shelf bank erosion [*Guo et al.*, 2007], both of which could lead to a remobilization of terrigenous particulate organic matter to the Arctic shelves. As a result, the increased inputs of DOC and POC will stimulate microbial respiration and, thus, increase DIC concentrations in the SML, increase fCO_2-sw and reduce CO_2 uptake rate by the ocean. Moreover, during extended ice-free periods, photo-oxidation of colored dissolved organic matter (CDOM) by UV radiation could increase the DIC concentration [*Bélanger et al.*, 2006] and result in higher fCO_2-sw in the SML. In addition, a decrease in sea ice formation in areas away from the influence of rivers would decrease vertical stratification, allowing high fCO_2 subsurface waters to mix into the surface, reducing the CO_2 sink, as demonstrated by *Miller et al.* [1999] in the Greenland Sea.

[31] Despite temporal and spatial variations, surface waters of the southeastern Beaufort Sea, the Mackenzie Shelf and the Cape Bathurst Polynya were mostly undersaturated with respect to atmospheric CO_2. The whole study area acted as a small to moderate sink for atmospheric CO_2, depending on the wind speed and ice cover. On average, the FCO_2 (uncorrected for ice cover) was -9.1 ± 9.0 mmol m^{-2} d^{-1} whereas the FCO_2-ic was four times lower, i.e., -2.3 ± 3.5 mmol m^{-2} d^{-1}. The FCO_2 is in agreement with results of previous studies, but the uncertainty associated with it highlights the strong variability in the carbonate system parameters observed on the Mackenzie Shelf and the Cape Bathurst Polynya. Physical factors like vertical mixing and temperature variation play a significant role in controlling sea surface fCO_2 [*Murata and Takizawa*, 2003; *Bates*, 2006]. As the incidence and strength of upwelling events and halocline perturbations will presumably increase with the forecasted increased frequency and intensity of cyclones [*Yang et al.*, 2004] and the retreat of the perennial ice pack beyond the shelf break in the Arctic [*Carmack and Chapman*, 2003], the potential release of CO_2 from upwelling requires further attention.

[32] **Acknowledgments.** We thank the captains and crews of the CCGS *Amundsen* for a most enjoyable and productive expedition in the Beaufort Sea. We thank Nes Sutherland, Constance Guignard, Pascale Collin, Mike Arychuk, Owen Owens, and Geneviève Bernier for their care and perseverance in collecting and analyzing the DIC, TA, and pH samples at sea during the nearly 12 month expedition. Marty Davelaar provided invaluable technical and analytical support from shore and Jeremy Lawrence and Erin Arctander also assisted with sample analyses. Thanks must go to Y. Gratton and the CTD data acquisition group for these essential measurements and their calibrations. The geographical maps in this study were created with the ODV Software (R. Schlitzer, Ocean Data View, http://odv.awi.de/, 2009). We thank Akihiko Murata and an anonymous reviewer for their detailed and valuable comments. This study was funded through the CASES (Canadian Arctic Shelf Exchange Study) NSERC Network and a Canadian Fund for Innovation grant to support the upgrade and operation of the CCGS *Amundsen*, as well as additional financial contributions from the Canadian Coast Guard and the Strategic Science Fund of the Department of Fisheries and Oceans Canada.

References

Agnew, T., and S. Howell (2003), The use of operational ice charts for evaluating passive microwave ice concentration data, *Atmos. Ocean*, *41*(4), 317–331, doi:10.3137/ao.410405.

Anderson, L. G., and S. Kaltin (2001), Carbon fluxes in the Arctic Ocean-Potential impact by climate change, *Polar Res.*, *20*(2), 225–232, doi:10.1111/j.1751-8369.2001.tb00060.x.

Anderson, L. G., H. Drange, M. Chierici, A. Fransson, T. Johannessen, I. Skjelvan, and F. Rey (2000), Annual carbon fluxes in the upper Greenland Sea based on measurements and a box-model approach, *Tellus Ser. B*, *52*(3), 1013–1024.

Arrigo, K. R., and G. L. van Dijken (2004), Annual cycles of sea ice and phytoplankton in Cape Bathurst polynya, southeastern Beaufort Sea, Canadian Arctic, *Geophys. Res. Lett.*, *31*, L08304, doi:10.1029/2003GL018978.

Barber, D. G., and J. M. Hanesiak (2004), Meteorological forcing of sea ice concentrations in the southern Beaufort Sea over the period 1979 to 2000, *J. Geophys. Res.*, *109*, C06014, doi:10.1029/2003JC002027.

Bates, N. R. (2006), Air-sea CO_2 fluxes and the continental shelf pump of carbon in the Chukchi Sea adjacent to the Arctic Ocean, *J. Geophys. Res.*, *111*, C10013, doi:10.1029/2005JC003083.

Bates, N. R., S. B. Moran, D. A. Hansell, and J. T. Mathis (2006), An increasing CO_2 sink in the Arctic Ocean due to sea-ice loss, *Geophys. Res. Lett.*, *33*, L23609, doi:10.1029/2006GL027028.

Bélanger, S., H. Xie, N. Krotkov, P. Larouche, W. F. Vincent, and M. Babin (2006), Photomineralization of terrigenous dissolved organic matter in

Arctic coastal waters from 1979 to 2003: Interannual variability and implications of climate change, *Global Biogeochem. Cycles*, *20*, GB4005, doi:10.1029/2006GB002708.

Bellis, A. (2002), Spectrophotometric determination of pH in estuarine waters using Phenol Red, B.Sc. thesis, 53 pp., McGill Univ., Montreal, Que., Canada.

Benner, R., B. Benitez-Nelson, K. Kaiser, and R. M. W. Amon (2004), Export of young terrigenous dissolved organic carbon from rivers to the Arctic Ocean, *Geophys. Res. Lett.*, *31*, L05305, doi:10.1029/2003GL019251.

Byrne, R. H. (1987), Standardization of standard buffers by visible spectrometry, *Anal. Chem.*, *59*, 1479–1481, doi:10.1021/ac00137a025.

Carmack, E. C., and D. C. Chapman (2003), Wind-driven shelf/basin exchange on an Arctic shelf: The joint roles of ice cover extent and shelf-break bathymetry, *Geophys. Res. Lett.*, *30*(14), 1778, doi:10.1029/2003GL017526.

Carmack, E. C., and E. A. Kulikov (1998), Wind-forced upwelling and internal Kelvin wave generation in Mackenzie Canyon, Beaufort Sea, *J. Geophys. Res.*, *103*(C9), 18,447–18,458, doi:10.1029/98JC00113.

Carmack, E. C., and R. W. Macdonald (2002), Oceanography of the Canadian Shelf of the Beaufort Sea: A setting for marine life, Arctic, *55*, suppl. 1, 29–45.

Carmack, E. C., R. W. Macdonald, and S. Jasper (2004), Phytoplankton productivity on the Canadian Shelf of the Beaufort Sea, *Mar. Ecol. Prog. Ser.*, *277*, 37–50, doi:10.3354/meps277037.

Carson, M. A., J. N. Jasper, and F. M. Conly (1998), Magnitude and sources of sediment input to the Mackenzie Delta, *Northwest Territories, 1974–94, Arctic*, *51*(2), 116–124.

Cavalieri, D., M. Thorsten, and J. Comiso (2004), AMSR-E/Aqua Daily L3 25 km Brightness Temperature and Sea Ice Concentration Polar Grids V002, http://nsidc.org/data/docs/daac/ae_si12_12km_tb_sea_ice_and_snow.gd.html, Natl. Snow and Ice Data Cent., Boulder, Colo.

Clayton, T. D., and R. H. Byrne (1993), Spectrophotometric seawater pH measurements: Total hydrogen ion concentration scale calibration of m-cresol purple and at-sea results, *Deep Sea Res. Part I*, *40*, 2115–2129.

Comiso, J. C. (2003), Warming trends in the Arctic from clear sky satellite observations, *J. Clim.*, *16*, 3498–3510, doi:10.1175/1520-0442(2003)016<3498:WTITAF>2.0.CO;2.

Comiso, J. C., D. J. Cavalieri, C. I. Parkinson, and P. Gloersen (1997), Passive microwave algorithms for sea ice concentration: A comparison of two techniques, *Remote Sens. Environ.*, *60*, 357–384, doi:10.1016/S0034-4257(96)00220-9.

Comiso, J. C., C. L. Parkinson, R. Gersten, and L. Stock (2008), Accelerated decline in the Arctic sea ice cover, *Geophys. Res. Lett.*, *35*, L01703, doi:10.1029/2007GL031972.

Dickson, A. G. (1990), Standard potential of the reaction: $(AgCl_{(s)} + 1/2H_{2(g)} = Ag_{(s)} + HCl_{(aq)})$, and the standard acidity constant of the ion HSO_4^- in synthetic sea water from 273.15 to 318.15 K, *J. Chem. Thermodyn.*, *22*(2), 113–127, doi:10.1016/0021-9614(90)90074-Z.

Dickson, A. G., and C. Goyet (Eds.) (1994), *Handbook of Methods for the Analysis of the Various Parameters of the Carbon Dioxide System in Sea Water*, version 2, Dep. of Energy, Washington, D. C. (Available at http://andrew.ucsd.edu/co2qc/handbook.html.)

Dickson, A. G., and F. J. Millero (1987), A comparison of the equilibrium constants for the dissociation of carbonic acid in seawater media, *Deep Sea Res. Part A*, *34*(10), 1733–1743.

Droppo, I. G., D. Jeffries, C. Jaskot, and S. Backus (1998), The prevalence of freshwater flocculation in cold regions: A case study from the Mackenzie River Delta, *Northwest Territories, Canada, Arctic*, *51*, 155–164.

Else, B. G. T., T. N. Papakyriakou, M. A. Granskog, and J. J. Yackel (2008), Observations of sea surface fCO_2 distributions and estimated air-sea CO_2 fluxes in the Hudson Bay region (Canada) during the open water season, *J. Geophys. Res.*, *113*, C08026, doi:10.1029/2007JC004389.

Fairall, C. W., E. F. Bradley, J. E. Hare, A. A. Grachev, and J. B. Edson (2003), Bulk parameterization of air-sea fluxes: Updates and verification for the COARE algorithm, *J. Clim.*, *16*(4), 571–591, doi:10.1175/1520-0442(2003)016<0571:BPOASF>2.0.CO;2.

Fransson, A., M. Chierici, and Y. Nojiri (2009), New insights into the spatial variability of the surface water carbon dioxide in varying sea ice conditions in the Arctic Ocean, *Cont. Shelf Res.*, *29*(10), 1317–1328, doi:10.1016/j.csr.2009.03.008.

Galley, R. J., E. Key, D. G. Barber, B. J. Hwang, and J. K. Ehn (2008), Spatial and temporal variability of sea ice in the southern Beaufort Sea and Amundsen Gulf: 1980–2004, *J. Geophys. Res.*, *113*, C05S95, doi:10.1029/2007JC004553.

Goñi, M. A., M. B. Yunker, R. W. Macdonald, and T. I. Eglinton (2005), The supply and preservation of ancient and modern components of organic carbon in the Canadian Beaufort Shelf of the Arctic Ocean, *Mar. Chem.*, *93*(1), 53–73, doi:10.1016/j.marchem.2004.08.001.

Gosink, T. A., J. G. Pearson, and J. J. Kelley (1976), Gas movement through sea ice, *Nature*, *263*(5572), 41–42, doi:10.1038/263041a0.

Gosselin, M., M. Levasseur, P. A. Wheeler, R. A. Horner, and B. C. Booth (1997), New measurements of phytoplankton and ice algal production in the Arctic Ocean, *Deep Sea Res. Part II*, *44*(8), 1623–1644, doi:10.1016/S0967-0645(97)00054-4.

Goulden, M. L., et al. (1998), Sensitivity of boreal forest carbon balance to soil thaw, *Science*, *279*, 214–217, doi:10.1126/science.279.5348.214.

Guo, L., C.-L. Ping, and R. W. Macdonald (2007), Mobilization pathways of organic carbon from permafrost to arctic rivers in a changing climate, *Geophys. Res. Lett.*, *34*, L13603, doi:10.1029/2007GL030689.

Hassol, S. J. (2004), Impacts of a warming Arctic: Arctic Climate Impact Assessment, synthesis report, Cambridge Univ. Press, Cambridge, U. K. (Available at http://www.acia.uaf.edu/.)

Ho, D. T., C. S. Law, M. J. Smith, P. Schlosser, M. Harvey, and P. Hill (2006), Measurements of air-sea gas exchange at high wind speeds in the Southern Ocean: Implications for global parameterizations, *Geophys. Res. Lett.*, *33*, L16611, doi:10.1029/2006GL026817.

Intergovernmental Panel on Climate Change (2008), *Climate Change 2007: Synthesis Report. Contribution of Working Groups I, II and III to the Fourth Assessment Report of the Intergovernmental Panel on Climate Change*, edited by Core Writing Team et al., Geneva, Switzerland.

Jähne, B., K. O. Münnich, R. B. A. Dutzi, W. Huber, and P. Libner (1987), On the parameters influencing air-water gas exchange, *J. Geophys. Res.*, *92*(C2), 1937–1949, doi:10.1029/JC092iC02p01937.

Johannessen, O. M., E. Bjørgo, and M. W. Miles (1996), Global warming and the Arctic, *Sciences*, *271*, 129.

Johnson, K. M., K. D. Wills, D. B. Butler, W. K. Johnson, and C. S. Wong (1993), Coulometric total carbon dioxide analysis for marine studies: Maximizing the performance of an automated gas extraction system and coulometric detector, *Mar. Chem.*, *44*(2–4), 167–187, doi:10.1016/0304-4203(93)90201-X.

Kaltin, S., L. G. Anderson, K. Olsson, A. Fransson, and M. Chierici (2002), Uptake of atmospheric carbon dioxide in the Barents Sea, *J. Mar. Syst.*, *38*(1–2), 31–45, doi:10.1016/S0924-7963(02)00168-9.

Keeling, R. F., S. C. Piper, A. F. Bollenbacher, and J. S. Walker (2008), Atmospheric Carbon Dioxide Record from Point Barrow, Alaska, http://cdiac.ornl.gov/trends/co2/sio-bar.html, Carbon Dioxide Inf. Anal. Cent., Oak Ridge Natl. Lab., Oak Ridge, Tenn.

Kulikov, E. A., A. B. Rabinovich, and E. C. Carmack (2004), Barotropic and baroclinic tidal currents on the Mackenzie shelf break in the southeastern Beaufort Sea, *J. Geophys. Res.*, *109*, C05020, doi:10.1029/2003JC001986.

Laxon, S., N. Peacock, and D. Smith (2003), High interannual variability of sea ice thickness in the Arctic region, *Nature*, *425*, 947–949, doi:10.1038/nature02050.

Lewis, E., and D. W. R. Wallace (1998), Program developed for CO_2 system calculations, *Rep. ORNL/CDIAC-105*, Carbon Dioxide Inf. Anal. Cent., Oak Ridge Natl. Lab., Oak Ridge, Tenn. (Available at http://cdiac.esd.ornl.gov/oceans/co2rprt.html.)

Liss, P. S., and L. Merlivat (1986), Air-sea gas exchange rates: Introduction and synthesis, in *The Role of Air-Sea Exchange in Geochemical Cycling*, edited by P. Buat-Ménard, pp. 113–127, D. Reidel, Boston.

Loeng, H., et al. (2005), Marine systems, in Arctic Climate Impact Assessment, edited by C. Symon, L. Arris, and B. Heal, pp. 453–538, Cambridge Univ. Press, Cambridge, U. K.

Loose, B., W. R. McGillis, P. Schlosser, D. Perovich, and T. Takahashi (2009), Effects of freezing, growth, and ice cover on gas transport processes in laboratory seawater experiments, *Geophys. Res. Lett.*, *36*, L05603, doi:10.1029/2008GL036318.

Macdonald, R. W., E. C. Carmack, F. McLaughlin, K. Iseki, D. Macdonald, and M. O'Brien (1989), Composition and modification of water masses in the Mackenzie shelf estuary, *J. Geophys. Res.*, *94*(C12), 18,057–18,070, doi:10.1029/JC094iC12p18057.

Macdonald, R. W., S. M. Solomon, R. E. Cranston, H. E. Welch, M. B. Yunker, and C. Gobeil (1998), A sediment and organic carbon budget for the Canadian Beaufort Shelf, *Mar. Geol.*, *144*(4), 255–273, doi:10.1016/S0025-3227(97)00106-0.

Macdonald, R. W., F. A. McLaughlin, and E. C. Carmack (2002), Fresh water and its sources during the SHEBA drift in the Canada Basin of the Arctic Ocean, *Deep Sea Res. Part I*, *49*(10), 1769–1785, doi:10.1016/S0967-0637(02)00097-3.

McGillis, W. R., J. B. Edson, J. D. Ware, J. W. H. Dacey, J. E. Hare, C. W. Fairall, and R. Wanninkhof (2001), Carbon dioxide flux techniques performed during GasEx-98, *Mar. Chem.*, *75*(4), 267–280, doi:10.1016/S0304-4203(01)00042-1.

McGuire, A. D., L. G. Anderson, T. R. Christensen, S. Dallimore, L. Guo, D. J. Hayes, M. Heimann, T. D. Lorenson, R. W. Macdonald, and N. Roulet (2009), Sensitivity of the carbon cycle in the Arctic to climate change, *Ecol. Monogr.*, *79*(4), 523–555.

Mehrbach, C., C. H. Culberson, J. E. Hawley, and R. N. Pytkowicz (1973), Measurement of the apparent dissociation constants of carbonic acid in seawater at atmospheric pressure, *Limnol. Oceanogr.*, *18*, 897–907.

Miller, L. A., M. Chierici, T. Johannessen, T. T. Noji, F. Rey, and I. Skjelvan (1999), Seasonal dissolved inorganic carbon variations in the Greenland Sea and implications for atmospheric CO_2 exchange, *Deep Sea Res. Part II*, *46*(6–7), 1473–1496, doi:10.1016/S0967-0645(99)00031-4.

Miller, L. A., et al. (2002), Carbon distributions and fluxes in the North Water, 1998 and 1999, *Deep Sea Res. Part II*, *49*(22–23), 5151–5170, doi:10.1016/S0967-0645(02)00183-2.

Millero, F. J., J.-Z. Zhang, S. Fiol, S. Sotolongo, R. N. Roy, K. Lee, and S. Mane (1993), The use of buffers to measure the pH of seawater, *Mar. Chem.*, *44*(2–4), 143–152, doi:10.1016/0304-4203(93)90199-X.

Mosley, L. M., S. L. G. Husheer, and K. A. Hunter (2004), Spectrophotometric pH measurement in estuaries using thymol blue and m-cresol purple, *Mar. Chem.*, *91*(1–4), 175–186, doi:10.1016/j.marchem.2004.06.008.

Murata, A., and T. Takizawa (2003), Summertime CO_2 sinks in shelf and slope waters of the western Arctic Ocean, *Cont. Shelf Res.*, *23*(8), 753–776, doi:10.1016/S0278-4343(03)00046-3.

Payette, S., A. Delwaide, M. Caccianiga, and M. Beauchemin (2004), Accelerated thawing of subarctic peatland permafrost over the last 50 years, *Geophys. Res. Lett.*, *31*, L18208, doi:10.1029/2004GL020358.

Peterson, B. J., J. McClelland, R. Curry, R. M. Holmes, J. E. Walsh, and K. Aagaard (2006), Trajectory shifts in the Arctic and Subarctic freshwater cycle, *Science*, *313*(5790), 1061–1066, doi:10.1126/science.1122593.

Pickart, R. S. (2004), Shelfbreak circulation in the Alaskan Beaufort Sea: Mean structure and variability, *J. Geophys. Res.*, *109*, C04024, doi:10.1029/2003JC001912.

Pipko, I. I., I. P. Semiletov, P. Y. Tishchenko, S. P. Pugach, and J. P. Christensen (2002), Carbonate chemistry dynamics in Bering Strait and the Chukchi Sea, *Prog. Oceanogr.*, *55*(1–2), 77–94, doi:10.1016/S0079-6611(02)00071-X.

Robert-Baldo, G., M. J. Morris, and R. H. Byrne (1985), Spectrophotometric determination of seawater pH using phenol red, *Anal. Chem.*, *57*, 2564–2567, doi:10.1021/ac00290a030.

Semiletov, I., A. Makshtas, S.-I. Akasofu, and E. Andreas (2004), Atmospheric CO_2 balance: The role of Arctic sea ice, *Geophys. Res. Lett.*, *31*, L05121, doi:10.1029/2003GL017996.

Semiletov, I. P., I. I. Pipko, I. Repina, and N. E. Shakhova (2007), Carbonate chemistry dynamics and carbon dioxide fluxes across the atmosphere-ice-water interfaces in the Arctic Ocean: Pacific sector of the Arctic, *J. Mar. Syst.*, *66*(1–4), 204–226, doi:10.1016/j.jmarsys.2006.05.012.

Serreze, M. C., M. M. Holland, and J. Stroeve (2007), Perspective on the Arctic's shrinking sea-ice cover, *Science*, *315*, 1533–1536, doi:10.1126/science.1139426.

Shindell, D. T., R. L. Miller, G. A. Schmidt, and L. Pandolfo (1999), Simulation of recent northern winter climate trends by greenhouse-gas forcing, *Nature*, *399*, 452–455, doi:10.1038/20905.

Steffen, K., D. J. Cavalieri, J. C. Comiso, K. St. Germain, P. Gloersen, J. Key, and I. Rubinsein (1992), The estimation of geophysical paratmeters using passive microwave algorithms, in *Microwave Remote Sensing of Sea Ice*, edited by F. Carsey, pp. 202–231, AGU, Washington, D. C.

Stein, R. (2000), Circum-Arctic river discharge and its geological record: An introduction, *Int. J. Earth Sci.*, *89*(3), 447–449, doi:10.1007/s005310000110.

Stroeve, J., M. M. Holland, W. Meier, T. Scambos, and M. Serreze (2007), Arctic sea ice decline: Faster than forecast, *Geophys. Res. Lett.*, *34*, L09501, doi:10.1029/2007GL029703.

Stull, R. B. (1988), *An Introduction to Boundary Layer Meteorology*, 666 pp., Kluwer Acad., Dordrecht, Netherlands.

Sweeney, C., E. Gloor, A. R. Jacobson, R. M. Key, G. McKinley, J. L. Sarmiento, and R. Wanninkhof (2007), Constraining global air-sea gas exchange for CO_2 with recent bomb ^{14}C measurements, *Global Biogeochem. Cycles*, *21*, GB2015, doi:10.1029/2006GB002784.

Takahashi, T., J. Olafsson, J. G. Goddard, D. W. Chipman, and S. C. Sutherland (1993), Seasonal variation of CO_2 and nutrients in the high latitude surface oceans: A comparative study, *Global Biogeochem. Cycles*, *7*, 843–878, doi:10.1029/93GB02263.

Tremblay, J.-É., K. Simpson, J. Martin, L. Miller, Y. Gratton, D. Barber, and N. M. Price (2008), Vertical stability and the annual dynamics of nutrients and chlorophyll fluorescence in the coastal, southeast Beaufort Sea, *J. Geophys. Res.*, *113*, C07S90, doi:10.1029/2007JC004547.

Vallières, C., L. Retamal, P. Ramlal, C. L. Osburn, and W. F. Vincent (2008), Bacterial production and microbial food web structure in a large arctic river and the coastal Arctic Ocean, *J. Mar. Syst.*, *74*(3–4), 756–773, doi:10.1016/j.jmarsys.2007.12.002.

Venegas, S. A., and L. A. Mysak (2000), Is there a dominant timescale of natural climate variability in the Arctic?, *J. Clim.*, *13*, 3412–3434, doi:10.1175/1520-0442(2000)013<3412:ITADTO>2.0.CO;2.

Wanninkhof, R. (1992), Relationship between wind speed and gas exchange over the ocean, *J. Geophys. Res.*, *97*, 7373–7382, doi:10.1029/92JC00188.

Wanninkhof, R. (2007), The impact of different gas exchange formulations and wind speed products on global air-sea CO_2 fluxes, in *Transport at the Air-Sea Interface*, edited by C. S. Garbe, R. A. Handler, and J. Bernd, pp. 1–23, Springer, Berlin.

Wanninkhof, R., and W. R. McGillis (1999), A cubic relationship between air-sea CO_2 exchange and wind speed, *Geophys. Res. Lett.*, *26*(13), 1889–1892, doi:10.1029/1999GL900363.

Weiss, R. F. (1974), Carbon dioxide in water and seawater: The solubility of a non-ideal gas, *Mar. Chem.*, *2*(3), 203–215, doi:10.1016/0304-4203(74)90015-2.

Weiss, R. F., and B. A. Price (1980), Nitrous oxide solubility in water and seawater, *Mar. Chem.*, *8*, 347–359, doi:10.1016/0304-4203(80)90024-9.

Williams, W. J., E. C. Carmack, K. Shimada, H. Melling, K. Aagaard, R. W. Macdonald, and R. G. Ingram (2006), Joint effects of wind and ice motion in forcing upwelling in Mackenzie Trough, Beaufort Sea, Cont. *Shelf Res.*, *26*(19), 2352–2366, doi:10.1016/j.csr.2006.06.012.

Williams, W. J., H. Melling, E. C. Carmack, and R. G. Ingram (2008), Kugmallit Valley as a conduit for cross-shelf exchange on the Mackenzie Shelf in the Beaufort Sea, *J. Geophys. Res.*, *113*, C02007, doi:10.1029/2006JC003591.

Woodgate, R. A., K. Aagaard, J. H. Swift, K. K. Falkner, and W. M. Smethie Jr. (2005), Pacific ventilation of the Arctic Ocean's lower halocline by upwelling and diapycnal mixing over the continental margin, *Geophys. Res. Lett.*, *32*, L18609, doi:10.1029/2005GL023999.

Yang, J., J. Comiso, D. Walsh, R. Krishfield, and S. Honjo (2004), Storm-driven mixing and potential impact on the Arctic Ocean, *J. Geophys. Res.*, *109*, C04008, doi:10.1029/2001JC001248.

Yu, Y., G. A. Maykut, and D. A. Rothrock (2004), Changes in the thickness distribution of Arctic sea ice between 1958-1970 and 1993–1997, *J. Geophys. Res.*, *109*, C08004, doi:10.1029/2003JC001982.

Yunker, M. B., L. L. Belicka, H. R. Harvey, and R. W. Macdonald (2005), Tracing the inputs and fate of marine and terrigenous organic matter in Arctic Ocean sediments: A multivariate analysis of lipid biomarkers, Deep Sea Res. *Part II*, *52*(24–26), 3478–3508, doi:10.1016/j.dsr2.2005.09.008.

Zemmelink, H. J., B. Delille, J. L. Tison, E. J. Hintsa, L. Houghton, and J. W. H. Dacey (2006), CO_2 deposition over the multi-year ice of the western Weddell Sea, *Geophys. Res. Lett.*, *33*, L13606, doi:10.1029/2006GL026320.

B. Lansard and A. Mucci, GEOTOP, Department of Earth and Planetary Sciences, McGill University, 3450 University St., Montreal, QC H3A 2A7, Canada. (bruno.lansard@mail.mcgill.ca)

L. A. Miller, Centre for Ocean Climate Chemistry, Institute of Ocean Sciences, Fisheries and Oceans Canada, PO Box 6000, Sidney, BC V8L 4B2, Canada.

T. N. Papakyriakou, Centre for Earth Observation Science, Department of Environment and Geography, University of Manitoba, 125 Dysart Rd., Winnipeg, MB R3T 2N2, Canada.